Long-Term Consecutive DInSAR for Volume Change Estimation of Land Deformation

Josaphat Tetuko Sri Sumantyo, *Member, IEEE*, Masanobu Shimada, *Fellow, IEEE*, Pierre-Phillippe Mathieu, and Hasanuddin Zainal Abidin

***Abstract*—In this paper, the long-term consecutive differential interferometric synthetic aperture radar (SAR) technique is used to measure the volume change during land deformation. This technique was used to investigate the subsidence of Bandung city, Indonesia, by assessing the data from two Japanese L-band spaceborne SARs (Japanese Earth Resources Satellite 1 SAR and Advanced Land Observation Satellite Phased Array type L-band Synthetic Aperture Radar) during the periods of 1993–1997 and 2007–2010. The results are confirmed using GPS observation data, ground survey data, local statistics, ground water level trend data, and the geological formation of the study area. The obtained results reveal a close correlation between the subsidence measurements and changes in the ground water level due to water pumping, population growth, industry growth, and urbanization of the study area.**

***Index Terms*—Advanced Land Observation Satellite Phased Array type L-band Synthetic Aperture Radar (ALOS PALSAR), Differential Interferometric Synthetic Aperture Radar (DInSAR), Japanese Earth Resources Satellite-1 Synthetic Aperture Radar (JERS-1 SAR), subsidence, volume change.**

I. Introduction

THE Japan Aerospace Exploration Agency (JAXA), formerly known as National Space Development Agency of Japan, has operated two synthetic aperture radar (SAR) systems on board satellites, namely, the Japanese Earth Resources Satellite 1 Synthetic Aperture Radar (JERS-1 SAR) and the Advanced Land Observation Satellite Phased Array type L-band Synthetic Aperture Radar (ALOS PALSAR) [1], [2]. The JERS-1 SAR operated for a period of six years starting from April 15, 1992 and recorded ten of the satellite images (each image covers a 75 km $\times$ 75 km area) used in the present study. The SAR is an active sensor that can observe objects during the day or at night. Various methods to analyze SAR images have been developed in order to extract physical information such as interferometry, soil moisture, biomass, and soil-type data. The application of SAR sensors for Earth surface observation of, for example, land deformation, the cryosphere, agriculture, forestry, and ocean dynamics has also been proposed [3]–[10]. A number of methods have been developed to extract volume changes using a digital elevation model (DEM), a map-based topographic approach, a generalized triprism, and interferometric coherence. Moreover, interferometric SAR (InSAR) applications to determine the volume change caused by volcanic activity and ground water pumping in urban areas, for example, have been developed [11]–[17]. However, it is difficult to obtain high-precision volume change data associated with Earth surface deformation using these methods for long-term consecutive remotely sensed observations. Recently, a number of commercial differential InSAR (DInSAR) software packages have been released, and these are able to produce the phase difference as the output, including the unwrapped phase information. In this paper, an equation is derived to determine the volume change on the surface of the Earth using the DInSAR technique or the phase difference. We apply this equation to long-duration measurement data and investigate the correlation between the subsidence measurements and changes in the ground water level due to water pumping, growth in population, industry, and urbanization of Bandung city, Indonesia.

The remainder of this paper is organized as follows. Section II describes the volume change estimation due to land deformation. Section III describes the DInSAR processing method. The study area is presented in Section IV. Consecutive satellite images are described in Section V. The results and a discussion are presented in Section VI. Finally, conclusions are presented in Section VII.

II. Volume Change Estimation Due To Land Deformation

In this paper, we implemented the phase information of two complex data as DInSAR data [18]–[22] to retrieve the volume change caused by long-term consecutive land surface deformation, particularly subsidence or uplift. Fig. 1 shows the geometry of the DInSAR for volume change or land

Manuscript received December 3, 2009; revised July 11, 2010, December 28, 2010, and March 27, 2011; accepted June 12, 2011. Date of publication August 4, 2011; date of current version December 23, 2011. This work was supported in part by the European Space Agency Earth Observation Category 1 under Grant 6613 through the framework of the "Long-Term Consecutive DInSAR for Land Deformation Monitoring" project, by the Japan Society for the Promotion of Science through a Grant-in-Aid for Scientific Research for Young Scientists (A) under Grant 19686025 and a Grant-in-Aid for Scientific Research under Grant 19-07023, and by the National Institute of Information and Communication Technology of Japan through an International Research Collaboration Research Grant 2008. This work was also supported in part by a Research Grant for Mission Research on a Sustainable Humanosphere from the Research Institute for a Sustainable Humanosphere, Kyoto University, Japan, and in part by Remote Sensing Research Center, Pandhito Panji Foundation, Bandung, Indonesia.

J. T. Sri Sumantyo is with the Center for Environmental Remote Sensing, Chiba University, Chiba 263-8522, Japan (e-mail: jtetukoss@faculty.chiba-u.jp).

M. Shimada is with the Earth Observation Research Center, Japan Aerospace Exploration Agency, Tsukuba 350-8505, Japan (e-mail: shimada.masanobu@jaxa.jp).

P. P. Mathieu is with the Department of Earth Observation Science and Applications, European Space Research Institute, European Space Agency, 00044 Frascati, Italy (e-mail: Pierre.Philippe.Mathieu@esa.int).

H. Z. Abidin is with the Department of Geodesy, Institute of Technology Bandung, Bandung 40132, Indonesia (e-mail: hzabidin@gd.itb.ac.id).

Digital Object Identifier 10.1109/TGRS.2011.2160455

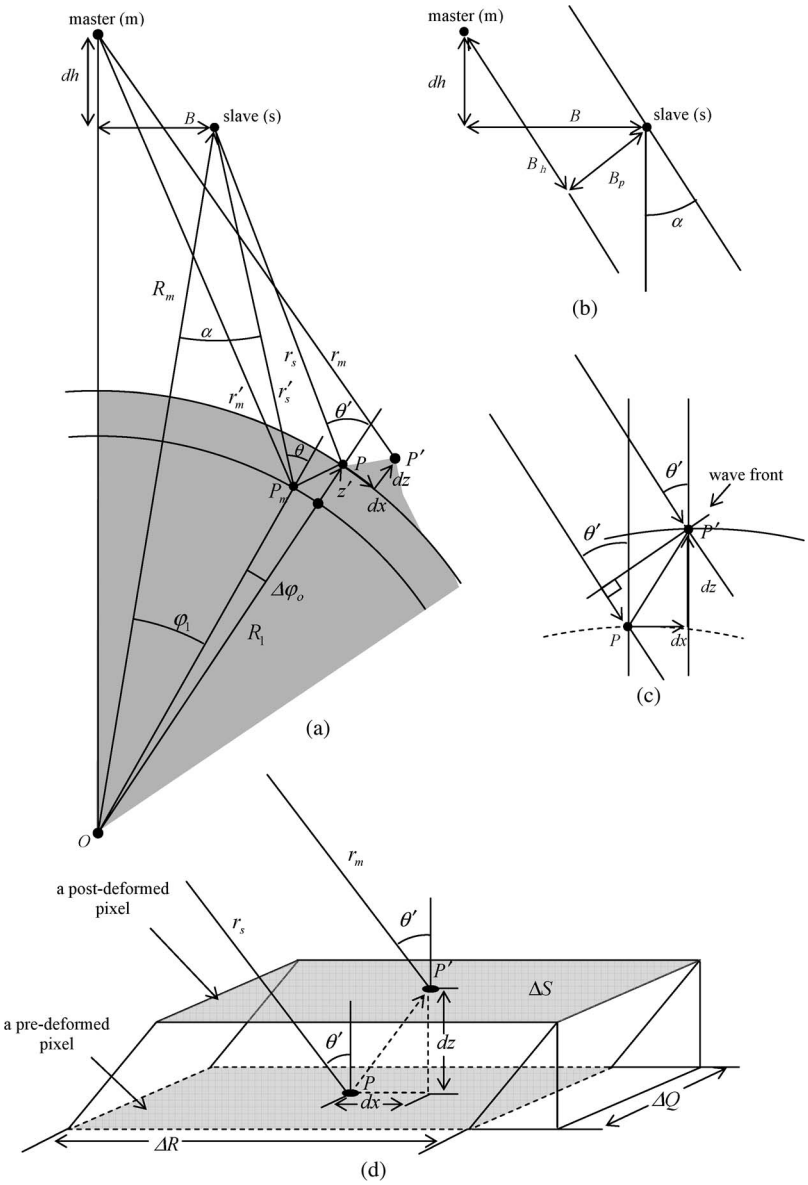

Fig. 1. Geometry of DInSAR. (a) Geometry of DInSAR for land deformation (uplift). (b) Geometry of baselines. (c) Geometry of land deformation on the surface of the Earth (uplift). (d) Geometry of pixel-based volume change.

deformation (in this case, uplift). Fig. 1(d) shows a pixel model of land deformation used to determine the volume change in a pixel. Based on Fig. 1, we obtained the total deformed volume of a pixel, which is acquired as

$$V_{m,n} = \Delta S \left[\frac{1}{\cos\theta'_{m,n}} \left\{ \frac{z'_{m,n} B_p}{r_m \sin\alpha_{m,n}} + \frac{\lambda \phi_{m,n}}{4\pi} - B_h \right\} \right] \quad (1)$$

where m and n indicate the line and row of the pixel in the SAR image. λ is the wavelength, B_h and B_p are the horizontal and perpendicular baseline distances, $\alpha_{m,n}$ is the off-nadir angle, $\theta'_{m,n}$ is the incidence angle on a deformed pixel, and r_m is the slant range. In addition, $z'_{m,n}$ is the topographical information and $\phi_{m,n}$ is the phase difference (postunwrapping phase). In this paper, we assume only land deformation in the vertical direction (uplift or subsidence) d_z, and the horizontal deformation d_x is neglected. A list of parameters for JERS-1 SAR and ALOS PALSAR used in the present study is presented in Table I. The size of the pixel surface area is obtained by multiplying the spatial resolutions along the ground range and azimuth directions: $\Delta S = \Delta R \Delta Q$; see Fig. 1(d).

Commercial DInSAR software often gives only the phase difference. Therefore, we can substitute the phase difference or the phase information output for each pixel into (1) to obtain the volume change of the targeted area.

III. DInSAR Processing

In the present study, the raw SAR data were processed using JAXA/SIGMA SAR software, which was developed by Shimada [19], to derive the interferogram or phase difference and the parameters in (1), in which the interferograms of JERS-1 SAR image pairs and ALOS PALSAR image pairs discussed in this paper were resampled to a resolution of 12.5 m. Based on the definitions presented in the derivation of the

TABLE I
JERS-1 SAR AND ALOS PALSAR IMAGES USED IN THE PRESENT STUDY

Sensor Name (Pair Code)	(Slave) Center date/time (UTC) Center coordinate	(Master) Center date/time (UTC) Center coordinate	A/D	Path/Row (Frame)	B (km)	Bp (km)	α (deg)	dh (km)	dh⊥ (km)	dhpr (km)
JERS-1 SAR (J1)	19930408 03:07:30.900 -6.884 /107.480	19940326 03:04:00.1 -6.884 /107.498	D	106/312	1.700	-1.434	34.784	0.101	-1.434	-0.874
JERS-1 SAR (J2)	19940326 03:04:00.100 -6.884 /107.498	19950128 03:08:48.1 -6.882 /107.522	D	106/312	0.925	0.653	35.104	0.170	0.649	0.637
JERS-1 SAR (J3)	19950128 03:08:48.100 -6.882 /107.522	19960115 03:13:42.5 -6.884 /107.493	D	106/312	0.290	-0.116	35.219	-0.259	0.084	-0.377
JERS-1 SAR (J4)	19960115 03:13:42.500 -6.884 /107.493	19961118 03:13:54.6 -6.883 /107.506	D	106/312	0.023	-0.044	35.225	0.046	-0.045	0.025
JERS-1 SAR (J5)	19961118 03:13:54.600 -6.883 /107.506	19970809 03:13:41.1 -6.884 /107.495	D	106/312	0.573	-0.262	35.329	-0.329	-0.271	-0.595
ALOS PALSAR (A1)	20070114 15:40:58.378 -7.027/107.649	20080117 15:39:52.428 -7.019/107.658	A	436/7040	1.549	1.179	34.385	0.189	1.172	1.030
ALOS PALSAR (A2)	20080126 02:55:48.000 -7.030/107.718	20081213 02:56:20.170 -7.020/107.713	D	101/3760	0.803	0.714	34.354	-0.071	0.704	0.394
ALOS PALSAR (A3)	20081213 02:56:20.170 -7.020/107.713	20091216 02:58:49.532 -7.011/107.717	D	101/3760	0.307	-0.300	34.359	0.058	-0.286	-0.126
ALOS PALSAR (A4)	20091216 02:58:49.532 -7.011/107.717	20101103 02:55:49.732 -6.964/107.729	D	101/3760	0.029	-0.028	34.356	0.089	-0.026	0.090

equations in Section II and Fig. 1, the earlier observed image is used as the *slave*, and the most recent image is used as the *master*. The DInSAR processing in this software, initiated by the data pair, is implemented using the same Doppler centroid and the individual Doppler chirp rates, where the start address for the slave image is selected using the satellite telemetry to overlay the slave image onto the master data to the greatest degree possible. The master and slave images are then coregistered using two processing steps: coarse registration and fine registration. These data, which are then wrapped, normally contain the high-frequency parallel component generated by the horizontal baseline distance. This component should be eliminated using the orbital data, where orbit tuning is conducted by the following: 1) selecting ground control points (gcps) in the image, where the address (line and pixel) and height are prepared; 2) unwrapping the flat-Earth-corrected fringe; 3) generating the unwrapped fringe using the results from 2) and the orbital data; 4) determining differences in orbital height, horizontal baseline, and height change rate by minimizing the difference between the gcp altitude and the height from the unwrapped fringe. The preconditioned conjugate gradient method is used as the unwrapping technique, and the noise in the interferogram is filtered two or three times using a Goldstein and Werner filter [21], [22] to obtain a satisfactory interferogram.

In the DInSAR process, the simulated flat Earth was generated to correct the fringe using a Shuttle Radar Topography Mission (SRTM) DEM with a resolution of 90 m (SRTM 90m DEM) and the orbital data. The real and simulated flat-Earth-corrected fringes are then differentiated. Here, the difference in the coordinate system between the SRTM DEM and InSAR DEM is corrected locally on a point-by-point basis, where the segmented pseudoaffine transformation is used. Finally, the interferogram or phase difference image is obtained, and geocoded interferogram generation is then performed by cubic convolution interpolation of a Universal Transverse Mercator projection. Geographic information system (GIS) processing has been used to process, for example, interferograms, GPS observed data, statistics [23]–[25], geological data [26]–[34], ground survey data, digital maps [26], [35], and Japanese Army maps [36], in order to investigate the subsidence and its impact on the study area.

With respect to possible error sources in the DInSAR processing [19], there are primarily two types of errors, namely, random error and bias error, where the bias error is primarily generated by the temporal change of the atmosphere, orbital determination, and processing to correct the DEM for the detection of land deformation. Water vapor content often changes locally in the atmosphere and affects the local phase pattern appearing on the interferogram. The error in orbital information is also considered to reduce the accuracy of the interferogram. In the present study, orbital data correction was performed using the pattern of additional fringes that appeared in the interferogram, where this pattern appears as a simple function of the range and azimuth simulated using the DEM. This additional fringe pattern is a simulated pattern that was calculated using SRTM 90m DEM for orbital data correction of each pixel in the SAR data. In particular, this process is important in the processing of the JERS-1 SAR data, because the accuracy of the orbital data of JERS-1 SAR is lower than that of ALOS PALSAR. If accurate orbital data are obtained, then an accurate interferogram or phase difference can be obtained too. Finally, the volume change could be estimated accurately by substituting this phase difference into (1).

The zero level point for estimating the volume change obtained by the DInSAR method was selected as the GPS fixed point (reference station) or the Pascasarjana Office (PSCA) point (located at the Institute of Technology Bandung (ITB) complex, Indonesia) at coordinates 6.888073° S, 107.609049° E and height h ellipsoid of 813.233 m, as shown in Fig. 3. The level or height of this point is assumed to remain unchanged during the DInSAR observation period (1993–1997 and 2007–2010) and the GPS observation period (2000–2008).

IV. STUDY AREA: BANDUNG CITY, INDONESIA

A. Location of Bandung City

Bandung city is located in western Java island at a longitude of $107°10'48''-108°13'12''$ E and a latitude of $6°10'48''-7°44'24''$ S and is the capital of the province of

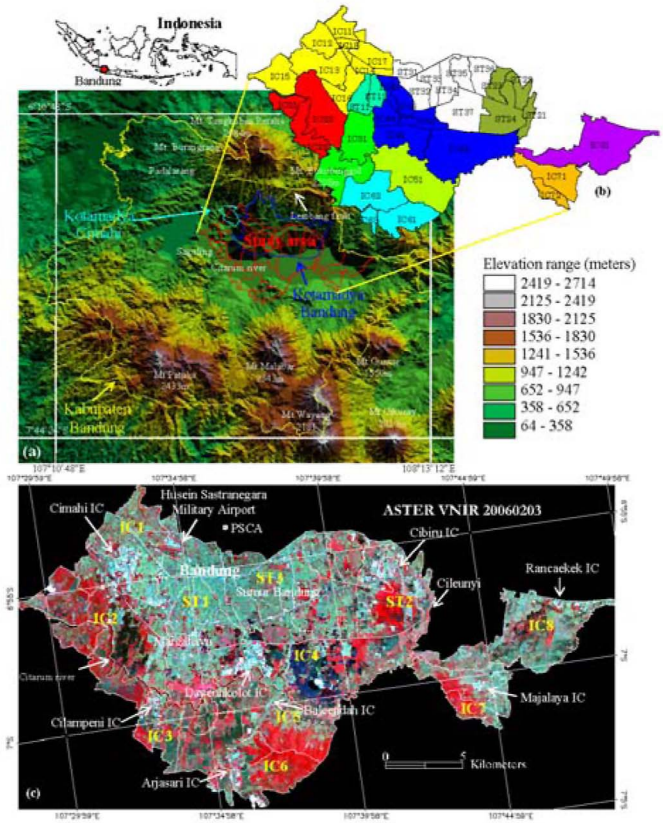

Fig. 2. Study area. (a) Study area, which covers part of Kotamadya Bandung, Kabupaten Bandung, and Kotamadya Cimahi. (b) Study area is determined by industrial and settlement areas that are affected by subsidence. (c) ASTER VNIR image (February 3, 2006), in which white areas indicate industrial complex (IC).

West Java, Indonesia [see Fig. 2(a)]. Topographically, the center of Bandung city is located at approximately 790 m above sea level. The highest point (2084 m) in this area is located in the north (Mount Tangkuban Perahu), and the lowlands in the south are approximately 64 m above sea level. The land in south Bandung is relatively flat, whereas the Bandung area is surrounded by mountains, creating Bandung basin. The Tangkuban Perahu and Bukit Tunggul mountains are located in the north, while the Patuha, Malabar, Guntur, Wayang, and Cikuray mountains are located in the south. The study area contains *Kotamadya* (municipality) Bandung, *Kabupaten* (Regency) Bandung, and *Kotamadya* Cimahi as shown in Fig. 2(a) with governmental boundaries shown by blue, yellow, and sea blue lines, respectively. The study area covers 345 km^2, as shown in Fig. 2(b). Fig. 2(c) shows the recent condition of the study area (Advanced Spaceborne Thermal Emission and Reflection Radiometer Visible Near Infrared acquired on February 3, 2006). The industrial areas (ICs) are shown in white and are distributed primarily in Cimahi (IC1), Soreang (IC2), Cilampeni (IC3), Dayeuhkolot (IC4), Balaendah (IC5), Arjasari (IC6), Majalaya (IC7), and Rancaekek (IC8) (see Fig. 2(b) and Table II). Residential areas (STs) are distributed in the Babakan Ciparay (ST1), Cileunyi (ST2), and Sumur Bandung (ST3) areas. The daily water supply in the study area often depends on ground water pumping using a man-made borehole or well, where the number of wells in the study area in 1995 is listed in Table II. People in this area use the ground water from wells for daily consumption, and many industries, such as textile and food industries, also consume ground water for industrial purposes. The distribution of surveyed wells or boreholes is shown in Fig. 3.

Based on a brief history of the study area, this city has grown rapidly after the Mataram Kingdom occupied this area and moved the capital from Krapyak, Dayeuhkolot, to the area now known as Bandung in 1641 [23]–[25], [34]. The climate of Bandung, which is influenced primarily by the mountains, is humid, and the average temperature is 24.5 °C. As shown in Fig. 2(b) and Table II, we classified eight industrial complexes (ICs) and three residential areas (STs) to analyze and investigate the effect of human and industrial activities on land deformation (subsidence) in the study area and the correlation between the subsidence measurements and changes in the ground water level due to water pumping, growth in population, industry, and urbanization of the study area. The area code, district code and name, coverage, population in 2008, and population density of each area are listed in Table II, which were compiled by the Indonesian Statistics Bureau (BPS) [23]–[25].

The location and number of boreholes are shown in Fig. 3 and Table II. The trend of the ground water level surveyed in 1980s, 1990s, and 2000s is also shown in Table II. This data reveal that the present ground water level is deeper compared to decades ago. The increase in the population and number of industries in this area is assumed to seriously affect the ground water level. Recently, a number of buildings and infrastructures (i.e., railway structures) in Bandung city were damaged, as shown in Fig. 4. The frequency of large-scale flooding also increased in some places [23]–[25] during the rainy seasons, which complicates the urban problems of this city. In the present study, the volume change is assessed numerically in order to estimate the amount of land deformation and map the area that suffered from subsidence. Long-duration DInSAR measurements are performed in order to investigate the correlation between the subsidence measurements and changes in the ground water level due to water pumping, growth in population, industry, and urbanization of the study area. In order to confirm this estimation, three ground surveys and six GPS observation surveys were performed, as explained in Section VI.

B. Population and Industry

The population trend from 1991 to 2008 in the study area is shown in Fig. 5. This population data were compiled, and GIS analysis was performed using the BPS data [23]–[25]. The population increased from 1991 to 2008 in industrial complexes as follows: from 102 940 to 169 484 at Cimahi Tengah (IC12), from 111 497 to 229 637 at Cimahi Selatan (IC13), from 118 881 to 182 455 at Cililin (IC21), from 99 598 to 147 584 at Soreang (IC22), from 71 555 to 114 510 at Margahayu (IC31), from 58 180 to 122 038 at Katapang (IC32), from 77 345 to 113 082 at Dayeuhkolot (IC41), from 97 932 to 178 060 at Baleendah (IC51), from 145 503 to 225 794 at Majalaya (IC71), and from 78 931 to 155 004 at Rancaekek (IC81). The data indicate that the Cimahi Selatan (IC13), Cililin (IC21), Baleendah (IC51), Majalaya (IC71), and Rancaekek (IC81)

TABLE II
CODE, COVERAGE, AND POPULATION OF THE INDUSTRIAL AND SETTLEMENT AREAS OF THE STUDY AREA

Area Code	District Code and Name		Coverage (km^2)	Population in 2008 (people)	Population Density in 2008 (people/km^2)	Ground Water Level in meters (number of surveyed boreholes)			Number of boreholes / wells in 1995
						1980s	1990s	2000s	
					Industrial Areas				
IC1	IC11	Cimahi Utara	13.32	137,622	10,332	9.5 (3)	23.0	25.0	25,001
	IC12	Cimahi Tengah	10.10	169,484	16,781	5.5 (12)	26.0	28.0	17,325
	IC13	Cimahi Selatan	16.94	229,637	13,556	12.5 (24)	44.0	48.0	23,735
	IC14	Andir	3.71	103,975	28,025	27.2 (6)	31.2	35.0	52,757
	IC15	Batujajar	83.68	106,724	1,275	- (2)	42.3	-	4,000
	IC16	Bandung Kulon	6.46	125,369	19,407	13.5 (16)	41.8	43.0	45,212
	IC17	Cicendo	6.86	99,452	14,497	16.0 (13)	27.4	31.0	52,757
	IC18	Sukajadi	4.30	100,244	2,382	- (0)	-	-	42,838
IC2	IC21	Cililin	81.55	182,455	2,237	- (0)	-	10.0	9,822
	IC22	Soreang	67.37	147,584	2,191	- (0)	-	-	8,334
	IC23	Margaasih	17.97	119,442	6,647	- (5)	29.0	30.0	35,431
IC3	IC31	Margahayu	10.54	114,510	10,864	4.8 (3)	8.15	12.0	7,611
	IC32	Katapang	21.16	122,038	5,767	5.75 (4)	30.85	32.0	7,438
IC4	IC41	Dayeuhkolot	11.03	113,082	10,252	8.5 (16)	34.0	36.0	7,178
	IC42	Bojongsoang	27.34	78,951	2,888	4.0 (3)	19.0	21.0	3,217
	IC43	Bandung Kidul	6.06	50,109	8,269	4.1 (4)	27.9	29.0	17,542
	IC44	Bojongloa Kidul	6.26	79,478	12,696	- (1)	17.9	20.0	39,148
	IC45	Astanaanyar	2.89	70,648	24,446	- (1)	5.4	7.0	27,827
	IC46	Regol	4.30	83,713	19,468	5.3 (1)	-	7.0	29,243
IC5	IC51	Baleendah	41.82	178,060	4,258	12.8 (6)	45.7	47.0	8,786
IC6	IC61	Arjasari	64.98	87,194	1,342	- (0)	-	-	3,346
	IC62	Pameungpeuk	14.62	62,634	4,284	6.82 (2)	-	-	4,833
	IC63	Banjaran	42.92	161,906	3,772	- (0)	-	-	8,551
IC7	IC71	Majalaya	25.36	225,794	8,904	- (3)	7.0	8.0	4,510
	IC72	Ciparay	46.18	142,008	3,075	- (1)	-	7.0	11,145
IC8	IC81	Rancaekek	45.30	155,004	3,421	4.3 (4)	18.2	20.0	6,158
					Settlement Areas				
ST1	ST11	Babakan Ciparay	7.45	137,392	18,442	14.0 (1)	-	16.0	53,254
	ST12	Bojongloa Kaler	3.03	118,898	39,240	4.7 (3)	17.1	18.0	37,426
ST2	ST21	Cileunyi	31.58	125,580	3,977	- (1)	-	10.0	3,968
	ST22	Cibiru	10.81	89,201	8,252	11.0 (4)	-	13.0	32,559
	ST23	Ujung Berung	10.34	84,931	8,214	9.1 (9)	20.4	23.0	39,927
	ST24	Rancasari	13.17	72,309	5,490	- (4)	13.3	15.0	30,927
ST3	ST31	Sumur Bandung	3.40	39,383	11,583	15.2 (9)	30.2	44.3	6,387
	ST32	Lengkong	5.90	72,059	12,213	18.0 (3)	26.6	28.0	13,740
	ST33	Batu Nunggal	5.03	122,345	24,323	9.5 (5)	32.2	35.0	52,757
	ST34	Kiara Condong	6.12	128,121	20,934	4.5 (4)	22.5	25.0	38,185
	ST35	Cicadas	8.66	108,245	12,499	15.5 (4)	22.9	25.0	34,115
	ST36	Arcamanik	8.80	68,860	7,825	12.5 (5)	28.8	30.0	26,243
	ST37	Margacinta	10.87	112,325	10,333	11.0 (7)	18.5	21.3	25,776

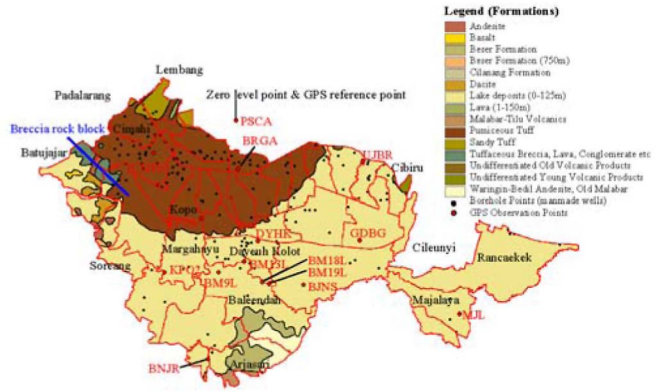

Fig. 3. Geological formation of the study area and location of borehole and GPS observation points.

Fig. 4. Sample photographs collected during a ground survey conducted on December 13–14, 2008, February 25–28, 2009, and August 4–10, 2009. Serious land subsidence affected the Cimahi, Dayeuhkolot, and Baleendah industrial complexes (IC1, IC4, and IC5). Cracked walls and roads were observed in residential, irrigation, and industrial infrastructures. The red, green, and blue arrows indicate vertical, diagonal, and horizontal cracking.

industrial areas have become highly populated. Table II and Fig. 5 show that the number of man-made wells or the amount of ground water pumping in the study area is strongly correlated with the population. Uncontrolled ground water pumping is considered to increase the subsidence of this area. The study area is composed primarily of pumiceous tuff and lake deposits (sediment) formed during the Pleistocene period, as shown in Fig. 3. This type of lithology is less stable than Breccia rock, which is distributed in the south at Cimahi Selatan (IC13). As a result, intense subsidence occurs in this area when ground water is pumped out in excess.

Fig. 6 shows the statistical data for the distribution of industry in the study area. We determine the number of industries as the total number of medium and large industries, which are defined as by the BPS to include industries with 20–99 employees and with more than 100 employees [23]–[25], respectively. As shown in Fig. 6, Cimahi Selatan (IC13), Bandung Kulon (IC16), Babakan Ciparay (ST11), Dayeuhkolot (IC41), Katapang (IC32), and Majalaya (IC71) are dense industrial areas having, respectively, 119, 59, 73, 70, 18, and 129 industrial sites in 1991 and 123, 58, 81, 73, 88, and 245 industrial sites in

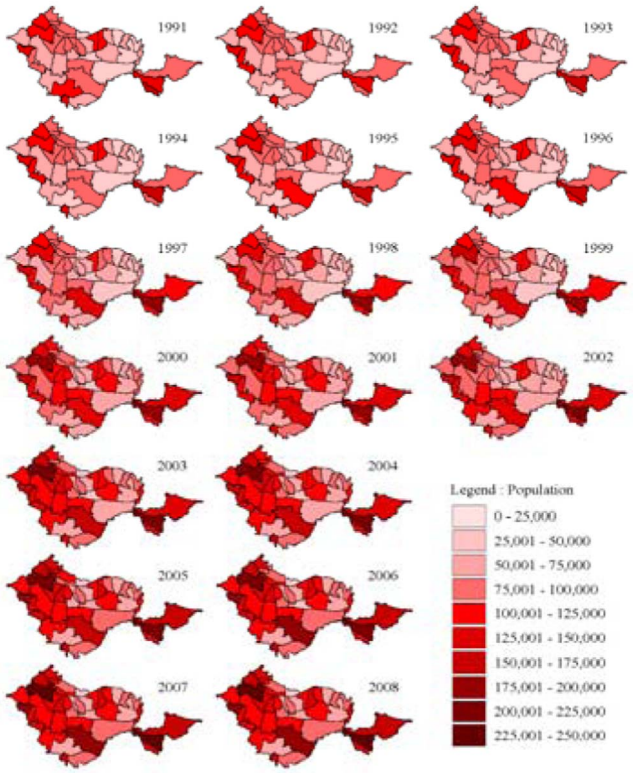

Fig. 5. Population of the study area from 1991 to 2008.

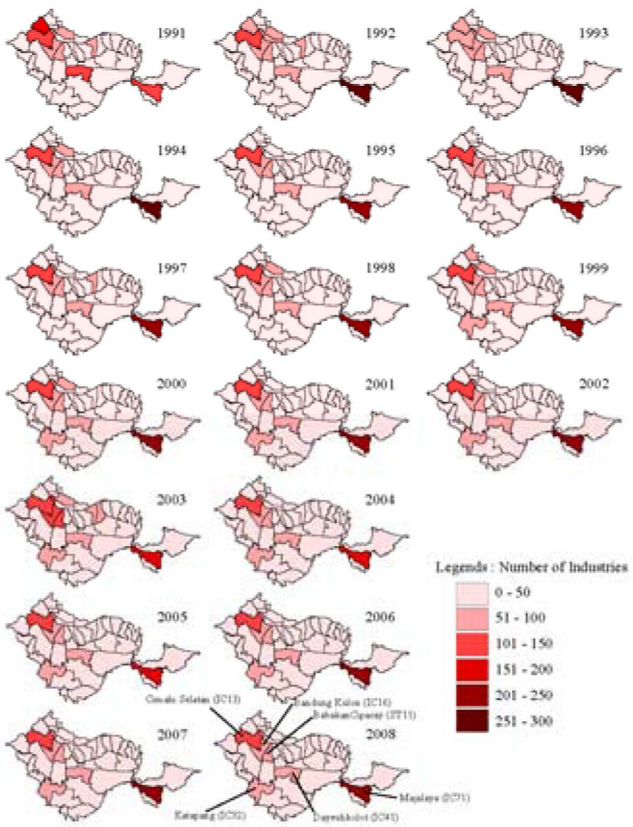

Fig. 6. Number of industries in the study area from 1991 to 2008.

2008. The industries are concentrated in the white area shown in Fig. 2(c). As mentioned earlier, uncontrolled ground water pumping and the unstable geological structure can deform the land surface significantly. This phenomenon is assumed to be caused by the increased frequency of flooding during the rainy season, which increases the ground water level (particularly in the dry season), which damages building and infrastructure in the study area, as shown in Fig. 4.

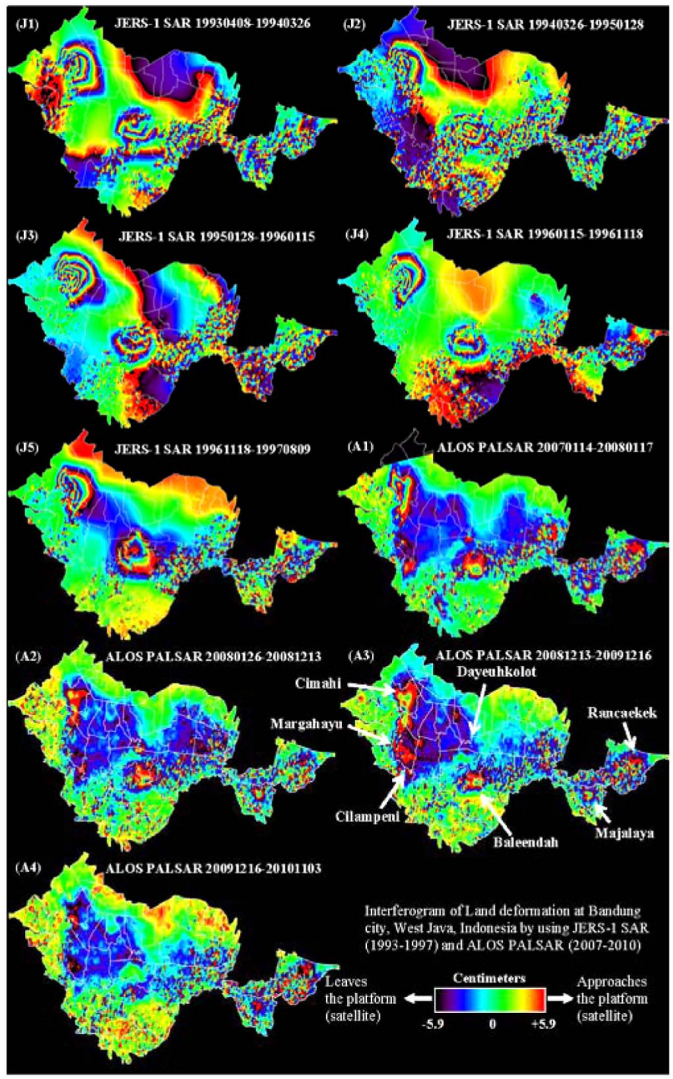

Fig. 7. Interferograms of the study area reveal that the main subsidence occurred in industrial areas, particularly Cimahi (IC1), Dayeuh Kolot (IC4), Baleendah (IC5), Arjasari (IC6), Majalaya (IC7), and Rancaekek (IC8).

V. Consecutive Satellite Images

In the present study, we implemented the DInSAR technique to determine the volume change due to land deformation at Bandung city over a long-term consecutive observation period. For this purpose, we use the Japanese L-band SAR sensors: JERS-1 SAR (1993–1997) and ALOS PALSAR (2007–2010). L-band microwaves can penetrate the vegetation canopy and reach the land surface [18]–[20]. Therefore, the land surface deformation can be more accurately observed using an L-band SAR sensor. Based on the definitions of the parameters of (1), as described in Section II, we use JERS-1 SAR pairs (pair number J1 to J5) and ALOS PALSAR pairs (pair number A1 to A4), as shown in Table I. The pairs exhibit consecutive periods during each mission (JERS-1 SAR:19930408-19940326-

TABLE III
MAXIMUM VALUE OF ESTIMATED SUBSIDENCE OF THE STUDY AREA (IN CENTIMETERS)

District Codes	District Name	Sensor Name and Data Combination (Slave - Master)								
		JERS-1 19930408-19940326	JERS-1 19940326-19950128	JERS-1 19950128-19960115	JERS-1 19960115-19961118	JERS-1 19961118-19970809	ALOS 20070114-20080117	ALOS 20080126-20081213	ALOS 20081213-20091216	ALOS 20091216-20101103
		Industrial Complexes								
IC1	Cimahi	55	45	57	47	36	21	10	15	10
IC2	Cililin	12	0	0	0	0	12	5	5	5
IC3	Margahayu	0	0	0	0	0	9	5	5	1
IC4	Dayeuhkolot	9	31	25	16	20	6	10	4	5
IC5	Baleendah	12	6	6	6	12	27	15	16	5
IC6	Arjasari	6	0	6	6	3	12	9	4	5
IC7	Majalaya	0	0	0	0	0	9	15	10	5
IC8	Rancaekek	12	0	0	0	9	9	5	5	5
		Settlement Areas								
ST1	Babakan Ciparay	12	6	6	3	3	3	5	5	4
ST2	Cileunyi	9	6	9	4	4	4	5	9	5
ST3	Sumur Bandung	9	9	9	4	4	4	5	4	2

19950128- 19960115-19961118-19970809 and ALOS PALSAR: 20070114- 20080117/20080126-20081213-20091216-20101103).

Therefore, the accumulation of consecutive volume changes due to subsidence in each district can be determined by substituting the phase difference of each pixel in the image and the appropriate parameters into (1). We also used 1:25 000 and 1:50 000 topographic maps, Japanese Army maps (Gaihozu) from Josaphat Laboratory archive, and other references [26]–[36] to analyze the study area, including geometric correction, geological information extraction, and confirmation of environmental changes.

VI. RESULTS AND DISCUSSION

A. DInSAR Results and Ground Survey Data Confirmation

Fig. 7 shows an interferogram of the long-term consecutive DInSAR results for each of the JERS-1 SAR and ALOS PALSAR pairs listed in Table I. In the interferogram (range: −5.9–5.9 cm), the cyan–blue–purple–black and cyan–green–yellow–red patterns indicate land surface movement away from (indicating subsidence) and toward (indicating uplift) the platform or spacecraft, respectively.

In order to confirm the real environmental condition of the study area, as shown in the interferogram in Fig. 7, we conducted three ground surveys on December 13–14, 2008, February 25–28, 2009, and August 4–10, 2009 in order to determine the conditions of buildings and infrastructure. Approximately 800 buildings were surveyed. Sample photographs of the buildings and infrastructure in the study area are shown in Fig. 4, where the coordinates in the figures indicate the position of each object.

The interferogram in Fig. 7 shows that the subsidence centered at the Cimahi Selatan industrial complex (IC13) significantly affected the surrounding area from 1993 to 2010. Subsidence occurred at industrial complexes [Cimahi Utara (IC11), Cimahi Tengah (IC12), Andir (IC14), Bandung Kulon (IC16), Cicendo (IC17), and Sukajadi (IC18)] and residential areas [Babakan Ciparay (ST11)]. Fig. 2(b) and Table II show the district codes and names. Husein Sastranegara Military Airport near Cimahi (IC1) and Sulaiman Airbase near Margahayu or Cilampeni (IC3) are also affected by the subsidence centered at Cimahi Selatan. If subsidence acts continuously in these areas, serious problems can occur that will eventually destroy the city infrastructure, e.g., the Indonesian aircraft industry in the Husein Sastranegara Military Airport complex, railway and road networks, and a newly developed residential area in Kopo city. As shown in Fig. 4(a), the ground surveys reveal damage to several walls in the residential area around the center of the subsidence at Cimahi Selatan (IC13). The walls of some buildings in this area exhibit cracks in the horizontal (blue arrow) and vertical (red arrow) directions. Land deformation in the horizontal and vertical directions is considered to be responsible for such damage, which is conspicuous in the buildings at the center of the subsidence at Cimahi Selatan (IC13). A number of houses were also found to be in the subsided condition (approximately 1 m), as shown in Fig. 4(b), which shows a house located near the center of the subsidence at Cimahi Selatan, which exhibited a maximum subsidence of 57 cm in 2005 (see Table III). The maximum subsidence in Table III is estimated using the DInSAR data, as explained in Section III. Significant subsidence occurred during 1993 and 1996 but decreased during the period from 1996 to 2010.

During the ground survey, we found that the soil type of this area is unstable pumiceous tuff and swamp (see Fig. 3). Therefore, the surrounding residential area is at risk of subsidence and other land deformations. Other public infrastructure, such as irrigation networks and roads, in Cimahi Selatan (IC13) was also found to be damaged, as shown in Fig. 4(c).

The interferogram also shows that subsidence occurred widely at Dayeuhkolot (IC4) during the period from 1993 to 1997, but this subsidence declined during the period from 2007 to 2010. On the other hand, subsidence occurred in other industrial complexes, namely, Margahayu or Cilampeni (IC3) and Baleendah (IC5), or south of Dayeuhkolot, at Majalaya (IC7) and Rancaekek (IC8), particularly during the period from 2007 to 2010, as shown in the interferogram in Fig. 7. The ground survey data show that the walls of buildings and concrete or asphalt road surfaces at Dayeuhkolot (IC4) were cracked, as shown in Fig. 4(d) and (e). The railway infrastructure in Baleendah area (IC5) was also found to be horizontally folded, as shown in Fig. 4(f). This condition worsened the urban problems in this area due to flooding during the rainy season. Based on the ground survey and interviews of the local people, the Citarum river at the boundary between Dayeuhkolot and Baleendah [see Fig. 2(c)] recently flooded to a level approximately 2 m higher than 20 years ago. Based on the DInSAR observations (a nine-year period) shown in Table III, Dayeuhkolot and Baleendah

subsided approximately 126 and 105 cm, respectively. This result is in approximate agreement with the present conditions of the study area.

As shown in Fig. 6, in 1991, the numbers of industries at Cimahi Selatan (IC13), Bandung Kulon (IC16), Babakan Ciparay (ST11), Dayeuhkolot (IC41), Katapang (IC32), and Majalaya (IC71) were 119, 59, 73, 70, 18, and 129, respectively. In 2008, this changed to 123, 58, 81, 73, 88, and 245 industries, respectively. This shows that the number of industries increased at Cimahi Selatan, Babakan Ciparay, Dayeuhkolot, Katapang, and Majalaya. On the other hand, the number of industries at Bandung Kulon (IC16) remained almost the same.

Increasing the number of industries is commonly followed by an increase in the number of employees, who settle around industrial sites. The increase in the number of industries is one reason for urbanization and the increase in population in the study area. The increases in industry and population will boost ground water pumping, which causes extensive subsidence in the study area. The ground water level (see Table II) at Cimahi Selatan, Bandung Kulon, Babakan Ciparay, Dayeuhkolot, Baleendah, Katapang, and Majalaya increased by 35.5, 29.5, 2, 27.5, 34.2, 26.25, and 8 m, respectively, from the 1980s to the 2000s. This indicates that the ground water level changed drastically at Cimahi Selatan, Bandung Kulon, Dayeuhkolot, and Baleendah districts, where the population densities in these areas are 13 556, 19 407, 10 252, and 4284 people/km^2. The man-made borehole or well densities in these areas are 10, 3, 16, and 20 people/well, respectively. This result reveals that the urbanization is concentrated in industrial areas because of uncontrolled ground water pumping or water consumption, which, in turn, caused the subsidence in the study area.

Based on the analysis of JERS-1 SAR data (1993–1997) and ALOS PALSAR data (2007–2010) shown in Fig. 7, the center of the subsidence at Dayeuhkolot shifted to Baleendah. The statistics reveal that the number of industries at Dayeuhkolot was 68 units in 1993, peaked at 76 units in 2003, and then decreased to 73 units in 2008. On the other hand, the number of industries at Baleendah was five units in 1993, peaked at 15 units in 2001, and 14 units are currently being operated. The population density and man-made well density are also high in Baleendah in the 2000s. The reason for this is assumed to be that the subsidence center moved from Dayeuhkolot in the 2000s and continues to occur extensively in Baleendah.

Fig. 7(A1)–(A4) shows that new subsidences occurred in the Margahayu–Cilampeni and Rancaekek areas in the 2000s, where the fluctuation of maximum subsidence is shown in Table III. The number of industries in Margahayu and Rancaekek was 17 and 15 units, respectively, in 1991 and was recently 43 and 30 units, respectively. The man-made well densities in these districts are 15 and 25 people/well, and the population densities are 10 864 and 3421 people/km^2. These results reveal that subsidence is occurring in areas with man-made well densities greater than ten.

An interesting phenomenon was observed at the Batujajar (IC15), Cililin (IC21), Soreang (IC22), and Margaasih (IC23) areas and the south of the Cimahi Selatan area. The subsidence is noticeably reduced due to the presence of a strong geological

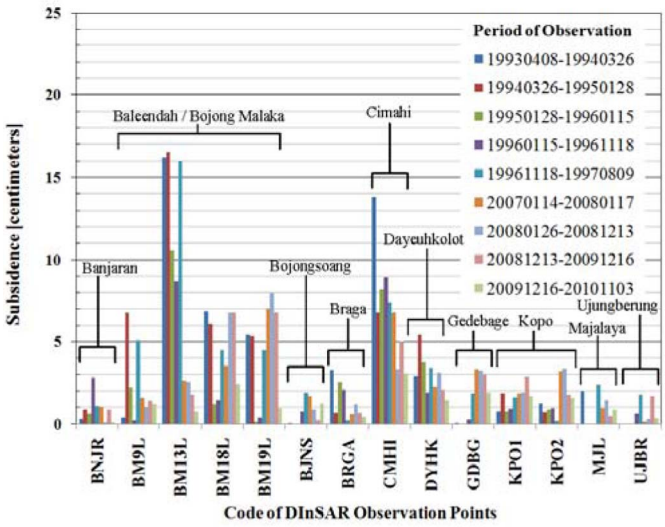

Fig. 8. Subsidence at each GPS observation point retrieved by ground observation from 2000 to 2008.

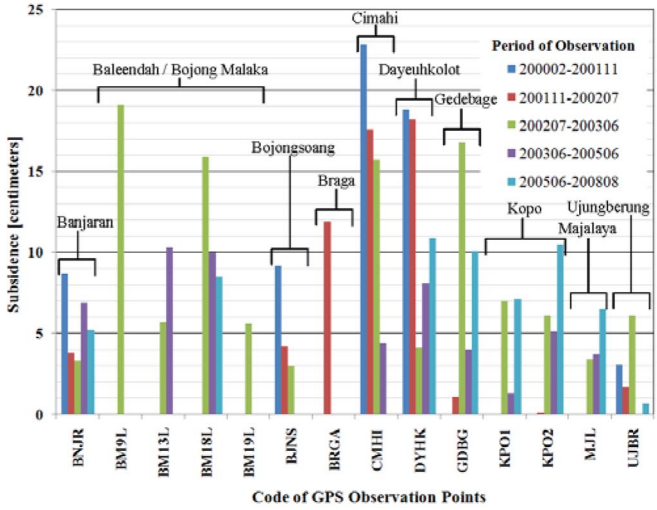

Fig. 9. Subsidence at each DInSAR observation point derived by DInSAR: Observation periods 1993–1997 and 2007–2010.

layer composed of tuffaceous breccias rock, lava, sandstone, and conglomerate, even though several industries and dense populations pumped out a significant amount of ground water in this southern area [see Figs. 2(c) and 3]. The largest subsidence, 57 cm, was observed to occur at the Cimahi area between January 28, 1995 and January 15, 1996. Recently, subsidence has continued to occur in Cimahi Selatan and the surrounding area, but the affected area is narrow compared to decades ago, and subsidence of approximately 10 cm occurred in 2010 (see Table III).

B. GPS Observation to Confirm the DInSAR Results

In order to confirm the DInSAR-derived phase difference that will be used for the calculations based on (1), we compared the vertical deformation or subsidence obtained by DInSAR and GPS observations. Six sets of GPS observations were conducted by H. Z. Abidin team [37], [38] to investigate the subsidence at the study area on February 21–24, 2000,

TABLE IV
COMPARISON OF DInSAR AND GPS OBSERVATIONS—SUBSIDENCE RATES (IN CENTIMETERS/YEAR)

Location Codes	Location Name	Coordinate (degrees)		Height *h*	Observations		
		Latitude	Longitude	Ellipsoid (m)	DInSAR (20070114-20081213)	GPS (20050624-20080823)	Error (cm)
BNJR	Banjaran	7.040	107.591	692.6110	0.6	1.7	1.1
BM9L	Bojong Malaka 9	6.985	107.598	683.8645	1.3	-	-
BM13L	Bojong Malaka 13	6.978	107.614	680.6877	2.6	-	-
BM18L	Bojong Malaka 18	6.991	107.626	682.1178	5.1	2.8	2.3
BM19L	Bojong Malaka 19	6.992	107.630	682.3632	7.5	-	-
BJNS	Bojongsoang	6.993	107.652	685.4108	1.3	-	-
BRGA	Braga	6.919	107.610	726.2273	0.9	-	-
CMHI	Cimahi	6.909	107.557	731.6004	5.0	-	-
DYHK	Dayeuhkolot	6.965	107.623	691.5718	2.7	3.6	0.9
GDBG	Gedebage	6.964	107.688	686.7990	3.3	3.4	0.1
KPO1	Kopo 1	6.951	107.587	704.5284	1.9	2.4	0.5
KPO2	Kopo 2	6.985	107.563	683.4918	3.3	3.5	0.2
MJL	Majalaya	7.011	107.752	687.7829	1.2	2.2	1.0
UJBR	Ujungberung	6.914	107.690	702.2434	0.2	0.2	0.0

November 21–30, 2001, July 11–14, 2002, June 1–3, 2003, June 24–27, 2005, and August 20–23, 2008, with the observation points shown in Fig. 3. These surveys used dual-frequency geodetic-type GPS receivers, the reference point of which was the GPS station inside the ITB complex (PSCA point in Fig. 3). This point is also used as the zero level point for the derivation of volume change using DInSAR. The length of each session was 10–12 h with 30 s intervals of data collection and 15° of elevation mask. The height differences between two consecutive survey epochs were calculated based on the estimation of ellipsoidal heights obtained from GPS processing. The results of the GPS observation at each station are shown in Fig. 8. The results reveal that serious subsidence occurred at five areas, namely, Cimahi (CMHI, IC13), Dayeuhkolot (DYHK, IC41), Gedebage (GDBG, ST24), Banjaran (BNJR, IC61), and Baleendah (BM18L, IC51), where the total subsidences between February 2000 and August 2008 for these areas were 60.5, 60.1, 32.0, 27.9, and 34.4 cm, respectively. This result will be used in the following to confirm the subsidence at each GPS observation point obtained using DInSAR.

Fig. 9 shows the subsidence at each DInSAR observation point obtained by DInSAR for observation periods from April 8, 1993 to August 9, 1997 (JERS-1 SAR) and from January 14, 2007 to November 3, 2010 (ALOS PALSAR). This observation shows that the total subsidences of Cimahi (CMHI, IC13), Dayeuhkolot (DYHK, IC41), Gedebage (GDBG, ST24), Banjaran (BNJR, IC61), and Baleendah (BM18L, IC51) areas are 63.3, 26.2, 13.6, 7.8, and 39.5 cm, respectively. Based on the GPS and DInSAR results, the rates of volume change of the most seriously affected areas of Cimahi, Dayeuhkolot, and Baleendah areas in pixel units (12.5 m $\times$ 12.5 m) are 12.0, 11.7, and 6.7 m^3/year based on GPS observations (2000–2008) and 11.0, 4.5, and 6.9 m^3/year based on DInSAR observations (1993–1997 and 2007–2010). Even though the GPS and DInSAR observation periods are different, they both indicate that the rate of volume change of the Cimahi, Dayeuhkolot, and Baleendah areas is very high. This also shows that the results obtained by DInSAR and GPS are similar, even though that the DInSAR result for Dayeuhkolot is very low. This error is assumed to be caused by the effects of multiscattering due to a high density of buildings around the observation area, which leads to decorrelation between the image pairs in the DInSAR data. The ground control point of GPS observation at the Dayeuhkolot area was located under a highway bridge, which is considered to affect the GPS observation data. This result indicates that the phase difference retrieved from DInSAR is available as an input parameter of (1) in order to determine the volume change. In the next section, we will assess the DInSAR results to obtain the volume change.

Table IV shows the subsidence rates in centimeters per year determined from the DInSAR and GPS observations for the periods January 14, 2007–December 13, 2008 and June 24, 2005–August 23, 2008, respectively, which were used to investigate the accuracy of DInSAR measurement by direct comparison of line-of-sight (LOS) deformation from DInSAR with the GPS vector deformation projected into the DInSAR LOS with the PSCA point (see Fig. 3) as the zero level point or the reference point of both observations. The time periods of DInSAR and GPS observations do not overlap exactly, leading to the errors shown in Table IV. The largest error (2.3 cm) appears for the Bojong Malaka 18 or Baleendah observation point. The subsidence in this area is extensive during the DInSAR observation period. Therefore, the nonoverlapping observation periods have a significant effect on the comparison results. The average error of the comparison in Table IV is approximately $\pm$0.8 cm or $\pm$1.2 m^3/year/pixel (pixel resolution of 12.5 m $\times$ 12.5 m). This error will affect the volume change estimation, as discussed in the following section.

C. Volume Change Derivation

In this section, we will assess the proposed technique to retrieve the volume change of the study area using the SAR data pairs. For example, let us consider the district of Cimahi Selatan (IC13) and its surrounding areas. The phase difference obtained using DInSAR, namely, the elevation, incidence angle, and other parameters (see Table I) of each pixel, is inserted into (1) in order to derive the volume change of each pixel. The extraction of the target district area is based on the distribution of the subsidence, as shown in Figs. 2(a) and 7. Therefore, the subsidence at Cimahi Selatan and its surrounding area during the period from April 8, 1993 to March 26, 1994 affected approximately 29.5 km^2 and 8 112 500 m^3 (estimated error: $\pm$226 560 m^3) of the subsided soil volume. A maximum subsidence volume of approximately 8 635 500 m^3 (estimated error: approximately $\pm$232 704 m^3) occurred during the period from January 28, 1995 to January 15, 1996 and affected an area of 30.3 km^2. The same manner of assessment

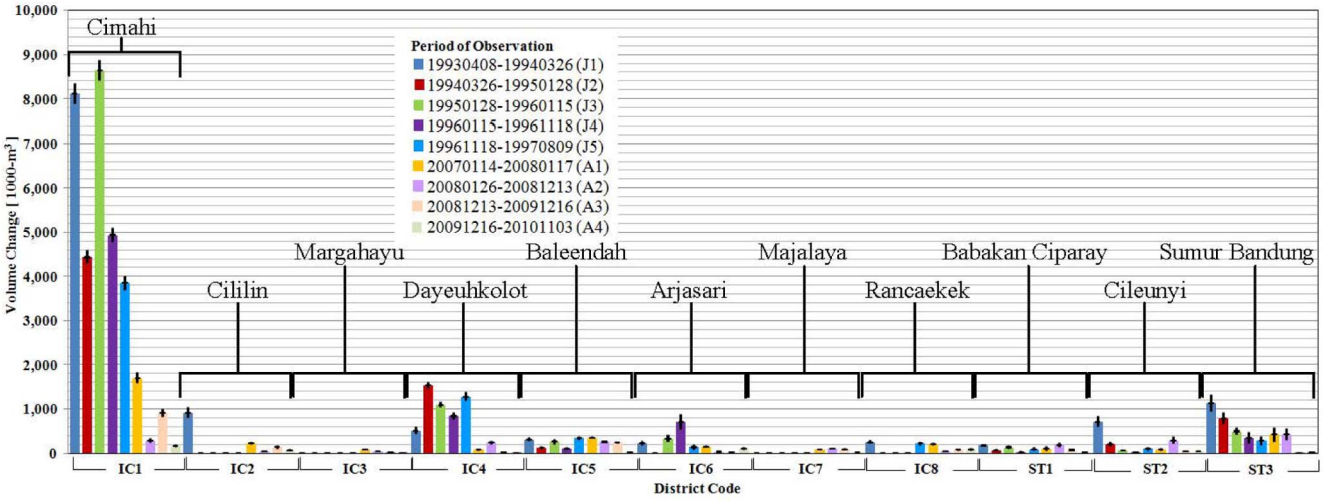

Fig. 10. Volume change of the study area derived by DInSAR observation during the periods of 1993–1997 and 2007–2010.

as that in the proposed technique is applied to the other areas, particularly Dayeuhkolot (IC41), Baleendah (IC51), Majalaya (IC71), and Rancaekek (IC81), and the detailed results are shown in Fig. 10. This figure shows the errors in volume change estimation in each district obtained using DInSAR. Based on the interferograms shown in Fig. 7, the subsidence phenomenon is continuously centered at the Cimahi Selatan, Dayeuhkolot, Majalaya, and Rancaekek industrial complexes and exhibits a decreasing trend, as shown in Fig. 10 and Table III. Subsidence was actively observed at the Baleendah, Majalaya, and Rancaekek areas during the monitoring period from January 14, 2007 to November 3, 2010 using ALOS PALSAR data. Some subsidence activities were also observed at Cilampeni industrial complex and the Katapang (IC32) and Margahayu (IC31) areas from 2007 to 2010. Figs. 5 and 6 show the effects of human and industrial activities in this area, and the overpumping of ground water is shown in Table II. These results were discussed in the previous section.

Geologically, the Dayeuhkolot, Baleendah, Katapang, Majalaya, and Rancaekek areas have unstable pumiceous tuff and lake deposits. This geological structure is assumed to be weak for industrial activities in these areas. On the other hand, the geological formation at Batujajar, Margaasih, and a small area of the southwest Cimahi Selatan area that is composed of tuffaceous breccias rock, lava, sandstone, and a conglomerate called breccia block (see Fig. 3) has a strong resistance to vertical land deformation, particularly subsidence.

VII. Conclusion

The DInSAR technique has been used to derive long-term consecutive volume changes at the surface of the Earth caused by land deformation (uplift or subsidence). In order to confirm the applicability of the DInSAR technique, we used this technique to investigate the subsidence in Bandung city, Indonesia, using JERS-1 SAR and ALOS PALSAR during the periods of 1993–1997 and 2007–2010. The results reveal that significant subsidence occurred at industrial complexes of Bandung city, particularly in the Cimahi, Dayeuhkolot, and Baleendah districts. The analysis results of ALOS PALSAR obtained using the proposed technique reveal new subsidence areas in industrial and residential areas of Majasari, Majalaya, Margahayu, Cilampeni, and Rancaekek. These results are confirmed by local statistical data published by the Statistics Bureau of Indonesia (BPS), GPS observations, ground surveys, the ground water level, and the geological formation of the study area. These results reveal a close correlation between the subsidence measurements and changes in the ground water level due to water pumping, growth in population, industry, and urbanization of the study area. They also allow the accuracy of the DInSAR measurements to be determined by direct comparison of LOS deformation from DInSAR with the GPS vector deformation projected into the DInSAR LOS. The resulting errors are approximately ± 0.8 cm or ± 1.2 m^3/year/pixel. This error affects the volume change estimation and must be considered when using the proposed method.

Acknowledgment

The authors would like to thank the reviewers for their valuable comments, B. Setiadi for conducting the second ground survey, I. Alimuddin for geological interpretation and geographic information system processing, and J. P. P. Herdento and I. I. Soekanto (Pandhito Panji Foundation) for collecting data statistics and old map collections. Japan Aerospace Exploration Agency SIGMA-SAR software was used to generate the interferograms used in the present study [21]. The authors would also like to thank the Japan Society of Instrument and Control Engineers (SICE) for SICE Award for this paper.

References

[1] M. Rossi, B. Rogron, and D. Massonnet, "JERS-1 SAR image quality and interferometric potential," *IEEE Trans. Geosci. Remote Sens.*, vol. 34, no. 3, pp. 824–827, May 1996.

[2] M. Shimada, "The overview of ALOS," *J. Remote Sens. Soc. Jpn.*, vol. 27, no. 4, pp. 394–396, 2007, (in Japanese).

[3] T. Strozzi, L. Tosi, P. Teatini, C. Werner, and U. Wegmuller, "Monitoring land subsidence within the Venice lagoon with SAR interferometry on trihedral corner reflectors," in *Proc. IEEE IGARSS*, Jul. 2009, vol. 4, pp. IV-33–IV-36.

[4] K. Ichikawa, T. Kozu, T. Shimomai, Y. Sakuno, T. Matsunaga, and K. Takayasu, "Estimation of coastal lagoon surface wind speed distribution using satellite SAR data," *J. Remote Sens. Soc. Jpn.*, vol. 28, no. 5, pp. 411–426, May 2009.
[5] T. R. Lauknes, A. Piyush Shanker, J. F. Dehls, H. A. Zebker, I. H. C. Henderson, and Y. Larsen, "Detailed rockslide mapping in northern Norway with small baseline and persistent scatterer interferometric SAR time series methods," *Remote Sens. Environ.*, vol. 114, no. 9, pp. 2097–2109, Sep. 2010.
[6] T. Deguchi, S. Rokugawa, and J. Matsushima, "Long-term ground deformation measurement by time series analysis for SAR interferometry," *J. Remote Sens. Soc. Jpn.*, vol. 29, no. 2, pp. 418–428, Oct. 2009.
[7] H. Balzter, C. S. Rowland, and P. Saich, "Forest canopy height and carbon estimation at Monks Wood National Nature Reserve, U.K., using dual-wavelength SAR interferometry," *Remote Sens. Environ.*, vol. 108, no. 3, pp. 224–239, Jun. 2007.
[8] E. S. Kasischke, L. L. Bourgeau-Chavez, A. R. Rober, K. H. Wyatt, J. M. Waddington, and M. R. Turetsky, "Effects of soil moisture and water depth on ERS SAR backscatter measurements from an Alaskan wetland complex," *Remote Sens. Environ.*, vol. 113, no. 9, pp. 1868–1874, Sep. 2009.
[9] T. Strozzi, R. Delaloye, A. Kaab, C. Ambrosi, E. Perruchoud, and U. Wegmuller, "Combined observations of rock mass movements using satellite SAR interferometry, differential GPS, airborne digital photogrammetry, and airborne photography interpretation," *J. Geophys. Res.*, vol. 115, p. F01 014, Mar. 2010. doi:10.1029/2009JF001311.
[10] R. Drews, W. Rack, C. Wesche, and V. Helm, "A spatially adjusted elevation model in dronning maud land, antarctica, based on differential SAR interferometry," *IEEE Trans. Geosci. Remote Sens.*, vol. 47, no. 8, pp. 2501–2509, Aug. 2009.
[11] A. B. Surazakov and V. B. Aizen, "Estimating volume change of mountain glaciers using SRTM and map-based topographic data," *IEEE Trans. Geosci. Remote Sens.*, vol. 44, no. 10, pp. 2991–2996, Oct. 2006.
[12] D. Che, L. Wu, and L. Xu, "Study on 3D modeling method of faults based on GTP volume," in *Proc. IEEE IGARSS*, Jul. 2006, pp. 1594–1597.
[13] L. E. B. Eriksson, M. Santoro, A. Wiesmann, and C. C. Schumullius, "Multitemporal JERS repeat-pass coherence for growing-stock volume estimation of Siberian forest," *IEEE Trans. Geosci. Remote Sens.*, vol. 41, no. 7, pp. 1561–1570, Jul. 2003.
[14] D. Myer, D. Sandwell, B. Brooks, J. Foster, and M. Shimada, "Inflation along Kilauea's southwest rift zone in 2006," *J. Volcan. Geotherm. Res.*, vol. 177, no. 2, pp. 418–424, Oct. 2008.
[15] Y. Fialko and M. Simons, "Evidence for on-going inflation of the Socorro magma body, New Mexico, from interferometric synthetic aperture radar imaging," *Geophys. Res. Lett.*, vol. 28, no. 18, pp. 3549–3552, Sep. 2001.
[16] F. Amelung, D. L. Galloway, J. W. Bell, H. A. Zebker, and R. J. Laczniak, "Sensing the ups and downs of Las Vegas: InSAR reveals structural control of land subsidence and aquifer-system deformation," *Geology*, vol. 27, no. 6, pp. 483–486, Jun. 1999.
[17] J. W. Bell, F. Amelung, A. R. Ramelli, and G. Blewitt, "Land subsidence in Las Vegas, Nevada, 1935–2000 : New geodetic data show evolution, revised spatial patterns, and reduced rates," *Environ. Eng. Geosci.*, vol. 8, no. 3, pp. 155–174, Aug. 2002.
[18] P. A. Rosen, S. Hensley, I. R. Joughin, F. K. Li, S. N. Madsen, E. Rodriguez, and R. M. Goldstein, "Synthetic aperture radar interferometry," *Proc. IEEE*, vol. 88, no. 3, pp. 333–382, Mar. 2000.
[19] M. Shimada, "A study on measurement of normalized radar cross section of earth surfaces by spaceborne synthetic aperture radar," Ph.D. dissertation, Tokyo Univ., Tokyo, Japan, Mar., 1999.
[20] M. A. Richards, "A beginner's guide to interferometric SAR concepts and signal processing," *IEEE Aerosp. Electron. Syst. Mag.*, vol. 22, no. 9, pp. 5–29, Sep. 2007.
[21] M. Shimada, "Verification processor for SAR calibration and interferometry," *Adv. Space Res.*, vol. 23, no. 8, pp. 1477–1486, 1999.
[22] R. M. Goldstein, H. A. Zebker, and C. L. Werner, "Satellite radar interferometry: Two-dimensional phase unwrapping," *Radio Sci.*, vol. 23, no. 4, pp. 713–720, Jul./Aug. 1988.
[23] Badan Pusat Statistik (BPS), Kotamadya Bandung Dalam Angka, (ISSN : 0215-2320, 32730–9301), Badan Pusat Statistik Kotamadya Bandung, Jan. 1991 $\sim$ Jan. 2008.
[24] Badan Pusat Statistik (BPS), Kabupaten Bandung Dalam Angka (ISSN 32060-9110, 0215-5265), Badan Pusat Statistik Kabupaten Bandung, Jan. 1990–Jan. 2008.
[25] Badan Pusat Statistik (BPS), Kota Cimahi Dalam Angka (BPS Catalog: 140-3204), Badan Pusat Statistik Kotamadya Cimahi, Jan. 2002–Jan. 2008.
[26] *Bandung Geological Digital Map*, LIPI Geoteknologi, Bandung, 2000.
[27] M. A. C Dam, "The late quaternary evolution of the Bandung basin, West, Java, Indonesia," Ph.D. dissertation, Vrije Universiteit, Amsterdam, The Netherlands, 1994.
[28] Puslitbang Geologi Bandung, Tangkuban Perahu, Direktorat Vulkanologi, Indonesia, 1974 , Puslitbang Geologi Bandung, Tangkuban Perahu, Direktorat Vulkanologi, Indonesia, 1974.
[29] R. P. Koesoemadinata, "Stratigrafi dan Sedimentasi Daerah Bandung," in *Proc. PIT X IAGI*, Bandung, Indonesia, Dec. 1981.
[30] C. H. E Stehn, *Volcanoes in the Bandung Region*. Bandung: Puslitbang Geologi, 1935.
[31] E. Sunardi, *Magnetic Polarity Stratigraphy of the Plio-Pleistocene Volcanic Rocks Around the Bandung, Basin, West Java, Indonesia*. Bandung: Puslitbang Geologi, 1996.
[32] R. W. Bemmelen, *The Geology of Indonesian*, vol. IA, *General Geology*. The Hague, The Netherlands: Martinus Nijhoff, 1949.
[33] S. Bronto and U. Hartono, "Potensi sumber daya geologi di daerah cekungan Bandung dan sekitarnya," *J. Geologi Indonesia*, vol. 1, no. 1, pp. 9–18, Mar. 2006.
[34] B. Brahmantyo and T. Bachtiar, *Wisata Bumi Cekungan Bandung—Jelajah Bandung Masa Lalu Dari Bentang Alam Masa Kini*. Indonesia: Truedee Pustaka Sejati, 2009.
[35] *Bakosurtanal, Topographic Maps : Padalarang (1209-224), Cililin (1209-222), Pasir Jambu (1208-544), Cimahi (1209-313), Bandung (1209-311), Soreang (1208-633), Lembang (1209-314), Ujung Berung (1209-312), Pakutandang (1208-634), Sukamulya (1209-323), Cicalengka (1209-321), and Majalaya (1208-643)*, I-2001 ed., Nat. Coordinating Agency Surv. Mapping (Bakosurtanal), Jakarta, Indonesia, 2001.
[36] Japanese Army, Old Japanese Military Maps: 84. Poerwakarta, 85. Tjikalongwetan, 86. Tjililin, 87. Goenoeng Patoeha, 88. Goenoeng Patengteng, 92. Tjiasem, 93. Lembang, 94. Bandoeng, 95. Bandjaran, 96. Pangalengan, 101. Soebang, 102. Boekit Toenggoel, 103. Goenoeng Poeloesari, 104. Tjiparaj (surveyed by Dutch Royal Army in 1910-1937), Japanese Army, 1943 (in Japanese and Dutch).
[37] H. Z. Abidin, H. Andreas, M. Gamal, A. D. Wirakusumah, D. Darmawan, T. Deguchi, and Y. Maruyama, "Land subsidence characteristics of the Bandung basin, Indonesia, as estimated from GPS and InSAR," *J. Appl. Geod.*, vol. 2, no. 3, pp. 167–177, Sep. 2008.
[38] H. Z. Abidin, H. Andreas, I. Gumilar, S. Wangsaatmaja, Y. Fukuda, and T. Deguchi, "Land subsidence and groundwater extraction in Bandung basin (Indonesia)," in *Proc. Symp. JS.2 Joint IAHS IAH Conv.—Trends and Sustainability of Groundwater in Highly Stressed Aquifers*, 2009, pp. 145–156, IAHS Publication No. 329.

Josaphat Tetuko Sri Sumantyo (S'00–A'02–M'04) was born in Bandung, Indonesia, on June 25, 1970. He received the B.Eng. and M.Eng. degrees in electrical and computer engineering (ground penetrating radar system) from Kanazawa University, Kanazawa, Japan, in 1995 and 1997, respectively, and the Ph.D. degree in artificial system sciences (applied radio wave and radar systems) from Chiba University, Chiba, Japan, in 2002.

He was a Researcher with the Indonesian Governmental Agency for Assessment and Application of Technology, Jakarta, and the Education and Training Commando (Kodiklat), Indonesian National Army (TNI-AD), Bandung and Baturaja, from 1990 to 1999. Since April 1, 2005, he has been an Associate Professor (permanent staff) with the Josaphat Microwave Remote Sensing Laboratory, Center for Environmental Remote Sensing, Chiba University, where he was a Research Assistant with the Center for Environmental Remote Sensing in 2000 and a Lecturer (Postdoctoral Fellowship Researcher) with the Center for Frontier Electronics and Photonics—Venture Business Laboratory from 2002 to 2005. He has been a Director with the Remote Sensing Research Center, Pandhito Panji Foundation, Indonesia, (www.pandhitopanji-f.org) since 2000. He is an Adjunct Professor and a Visiting Professor at the University of Indonesia, Depok, Indonesia; Institute of Technology Bandung; University of Udayana, Denpasar, Indonesia; and others. His main interests include microwave remote sensing [synthetic aperture radar (SAR)], SAR onboard small satellite and unmanned aerial vehicle, weather radar, scattering wave analysis and its applications, analysis of printed (microstrip), and carbon microcoil very small antennas for mobile satellite communications and microwave remote sensing, including microsatellite.

Dr. Sri Sumantyo is also a member of the Institute of Electronics, Information and Communication Engineers, Japan Society of Photogrammetry and Remote Sensing, and Remote Sensing Society of Japan. He was the recipient of many awards and research grants related to his study and research.

Masanobu Shimada (M'97–SM'04–F'11) received the B.S. and M.S. degrees in aeronautical engineering from Kyoto University, Kyoto, Japan, in 1977 and 1979, respectively, and the Ph.D. degree in electrical engineering from The University of Tokyo, Tokyo, Japan, in 1999.

He was with the National Space Development Agency (NASDA) of Japan, currently the Japan Aerospace Exploration Agency (JAXA), in 1979. During his time here, he designed a NASDA scatterometer. He served as a Visiting Scientist at the Jet Propulsion Laboratory in 1990. Since 1995, he has been with Earth Observation Research Center, JAXA, Tsukuba, Japan, where he is currently an Assistant Principal Researcher, has been assigned duties where he has served as the Advanced Land Observation Satellite (ALOS) Science Manager, responsible for ALOS calibration/validation, rainforest mapping projects, and synthetic aperture radar (SAR) interferometry projects, and where he developed data-processing subsystems for optical and SAR data (i.e., Marine Observation Satellite 1, Système Probatoire d'Observation de la Terre, and Japanese Earth Resources Satellite-1) from 1985 to 1995.

Pierre-Phillippe Mathieu received the B.S. degree in mechanical engineering and the M.Sc. degree from the University of Liege, Liege, Belgium, in 1994, the B.S. degree in management from the University of Reading Business School, Reading, U.K., in 2002, and the Ph.D. degree in oceanography from the Catholic University of Louvain, Louvain, Belgium, in 1998.

He is an Earth Observation Applications Engineer with the Department of Earth Observation Science and Applications, European Space Research Institute, European Space Agency, Frascati, Italy. He spent ten years working in the field of environmental modeling, weather risk management, and remote sensing.

Hasanuddin Zainal Abidin received the Ir. degree from the Institute of Technology Bandung, Bandung, Indonesia, in 1985 and the M.Sc.Eng. and Ph.D. degrees from the University of New Brunswick, Saint John, NB, Canada, in 1989 and 1992, respectively.

He is a Professor and Head of Geodesy Research Division, Faculty of Earth Science and Technology, Institute of Technology Bandung. His research interests include ambiguity resolution of Global Navigation Satellite System (GNSS) signals; use of space geodetic systems for monitoring fault motion, geodynamics, volcano deformation, land subsidence, landslide, and dam deformation; GNSS continuously operating reference station applications; and GNSS meteorology.

Prof. Abidin is a member of International Association of Geodesy, American Geophysical Union, and International Association of Hydrogeologists.